

BUTP-95/15
COLO-HEP-362

Non-perturbative tests of the fixed point action for $SU(3)$ gauge theory¹

Thomas DeGrand, Anna Hasenfratz
Department of Physics
University of Colorado, Boulder CO 80309-390

Peter Hasenfratz, Ferenc Niedermayer²
Institute for Theoretical Physics
University of Bern
Sidlerstrasse 5, CH-3012 Bern, Switzerland

June 1995

Abstract

In this paper (the second of a series) we extend our calculation of a classical fixed point action for lattice $SU(3)$ pure gauge theory to include gauge configurations with large fluctuations. The action is parameterized in terms of closed loops of link variables. We construct a few-parameter approximation to the classical FP action which is valid for short correlation lengths. We perform a scaling test of the action by computing the quantity $G = L\sqrt{\sigma(L)}$ where the string tension $\sigma(L)$ is measured from the torelon mass $\mu = L\sigma(L)$. We measure G on lattices of fixed physical volume and varying lattice spacing a (which we define through the deconfinement temperature). While the Wilson action shows scaling violations of about ten per cent, the approximate fixed point action scales within the statistical errors for $1/2 \geq aT_c \geq 1/6$. Similar behaviour is found for the potential measured in a fixed physical volume.

¹Work supported in part by Schweizerischer Nationalfonds, NSF Grant PHY-9023257 and U. S. Department of Energy grant DE-FG02-92ER-40672

²On leave from the Institute of Theoretical Physics, Eötvös University, Budapest

1 Introduction and summary

This paper is the second in a series [1] describing the construction and testing of a fixed point (FP) action for lattice $SU(3)$ pure gauge theory. In I we derived the general FP equations for the action and for selected operators. We discussed their properties on the classical level and in 1-loop perturbation theory. We solved the FP equation for the action and the Polyakov loop on fields with small fluctuations. The FP action is a perfect classical action on the lattice and, as we argued in I, it is perfect even in 1-loop perturbation theory. It is the $\beta = \infty$ point of the renormalized trajectory and, as such, will be the basic ingredient of future attempts to construct perfect actions. This should be the ultimate goal in order to reach the continuum limit without losing the battle against critical slowing down, memory problems and other theoretical or computational issues.

The aim of this paper is more modest. It is natural to expect, and this expectation is supported by a numerical study of the non-linear σ -model [2], that the FP action works much better than the Wilson action even at small correlation lengths. In this paper we perform a scaling test and make a comparison.

Scaling means that all physical dimensional quantities show the same functional dependence on the gauge coupling. It is different from asymptotic scaling where in addition to scaling we require that this functional dependence be described by the 2-loop Λ parameter. Asymptotic scaling properties can be significantly improved by a suitable non-perturbative redefinition of the bare coupling [3, 4]. In this paper we are not concerned with asymptotic scaling. Scaling properties can only be changed by modifying the lattice action. A redefinition of the coupling constant used in the lattice action during simulations will also shift parameters in the lattice action away from their naive free-field values. Simulations done with these new actions may show better scaling properties. An example of the use of such actions is the self-consistent tadpole-improvement program for nonrelativistic QCD which has been applied with great success to studies of charm and bottom quark systems[5].

Scaling violations can be different for different quantities. The ratio of certain observables might show scaling at smaller correlation length than others. Scaling requires the universal behavior of *all* observables. Of course, we cannot test all observables, but we can ask whether observables which show scaling violations when computed using the Wilson action scale better when using a FP action.

The first step is to derive a parametrization for the FP action which is sufficiently simple and approximates well the FP action on rough configurations

which typically enter our simulations. This is a multistep procedure which we discuss in some detail in Sections 2 and 3. At the end we obtained an 8 and a 16 parameter approximation of the FP actions for RG transformation of type I and type II, respectively. (These RG transformations were defined and discussed in detail in I.) These parametrizations are constructed in terms of two loops, the plaquette and the twisted perimeter-six loop. Powers of the real and the square of the imaginary part of the loop-trace enter the action with coefficients c_1, c_2, \dots and d_1, d_2, \dots , respectively as given in Tables 1 and 2.

Table 1: Couplings of the few-parameter FP action for the RG transformation of type I. The couplings d are zero.

operator	c_1	c_2	c_3	c_4
c_{plaq}	.523	.0021	.0053	.0167
c_{6-link}	.0597	.0054	.0051	-.0006

Table 2: Couplings of the few-parameter FP action for the RG transformation of type II.

operator	c_1	c_2	c_3	c_4	c_5
c_{plaq}	.6092	.0478	-.0470	.0295	-0.0038
c_{6-link}	.0489	-.0146	.0393	-.0216	.0039
operator	d_1	d_2	d_3		
c_{plaq}	.0921	-.1487	.0397		
c_{6-link}	.0042	-.0034	.0042		

We pushed the scaling test to the extreme, going to configurations with very large fluctuations (corresponding to Wilson $\beta = 5.1$). This extreme situation might be interesting for finding the connection with strong coupling expansions [6] but is, presumably, not practical in standard applications. On very rough configurations it is increasingly difficult to find a simple parametrization and, in addition, the correlation length is so small that the signal disappears rapidly.

In the scaling test which we performed with the 8 parameter action in Table 1, the critical temperature T_c was used to set the physical scale. We determined the critical coupling constant $\beta_c(N_t)$ for $N_t = 2, 3, 4$ and 6 (Table 6) and fixed the lattice spacing at these coupling values as $a = 1/(T_c N_t)$. The corresponding critical couplings for the Wilson action are known to good precision [7].

Next we measured physical observables at couplings $\beta_c(N_t)$ in fixed, finite physical volumes. This way we can avoid infinite volume extrapolations. For one scaling test we consider the quantity $G = L\sqrt{\sigma(L)}$ where $\sigma(L)$ is the string tension on an L^3 volume computed from the exponential fall-off of the Polyakov line correlator (torelon mass). Taking $L = rN_t$ where r is some conveniently

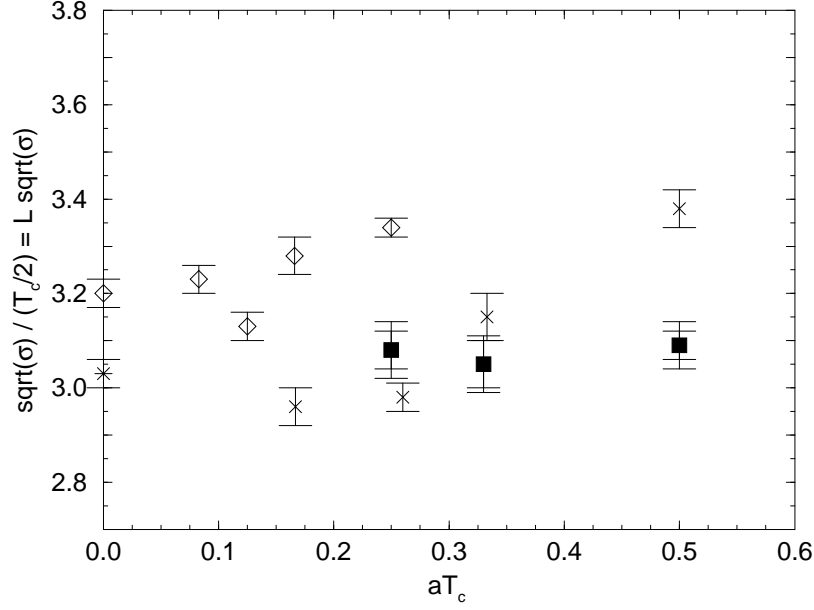


Figure 1: Scaling test for the Wilson action (crosses) and FP action (squares); T_c is defined in infinite spatial volumes. The diamonds are from zero-temperature simulations by Ref. 8 and the diamond and the star at $a = 0$ are extrapolations.

chosen aspect ratio, the physical volume is kept fixed at $V = (r/T_c)^3$. The ratio G is independent of the bare coupling (resolution) in the scaling (continuum) limit. Any variation of G is due to lattice artifacts. Figure 1 shows $G(L)$ with $r = 2$ as a function of aT_c for the Wilson and for the 8 parameter FP action. The inner and outer error bars on the FP points show their statistical uncertainty, and the combined uncertainty from statistics and in β_c . The Wilson action shows a scaling violation of about 10% between $N_t = 2$ and 6. No scaling violation above the statistical errors is seen for the FP action.

No simulations using the Wilson action at small lattice spacing precisely match our scaling test using the torelon mass on fixed physical volumes. The ones which come closest are the very recent ones of Boyd. et. al. [8]. These authors present measurements of the quantity $\sqrt{\sigma}/T_c$ at the critical couplings for $N_t = 4, 6, 8$, and 12, for which the string tension has been computed via fits to Wilson loops on large (zero temperature) lattices. (They also present new measurements of critical couplings at $N_t = 8$ and 12.) The string tension from Wilson loops is an upper bound on $\sigma(L)$; $\sigma(L)$ is reduced from σ by the zero-point fluctuation term which for large L in a string model is [9]

$$\sigma(L) = \sigma - \frac{\pi}{3L^2} + \dots \quad (1)$$

The diamonds in Fig. 1 show $2\sqrt{\sigma}/T_c$ from Ref. [8]. The authors of that work present an extrapolation to $a = 0$, which we also display along with the $a = 0$ limit of $L\sqrt{\sigma(L)}$ at $r = 2$ calculated from Eq. (1).

Torelon masses at small lattice spacing have been presented in the literature, but they are not at couplings which are critical couplings for deconfinement for integer N_t 's. Our attempts to interpolate them into scaling tests which match our simulations generally resulted in uselessly large uncertainties, and we do not show them here.

Results are similar from Fig. 2 where the aspect ratio $r = 3/2$ data are plotted. In both cases the question remains unanswered, whether the constant observed with the FP action at very low resolutions really agrees with the continuum value.

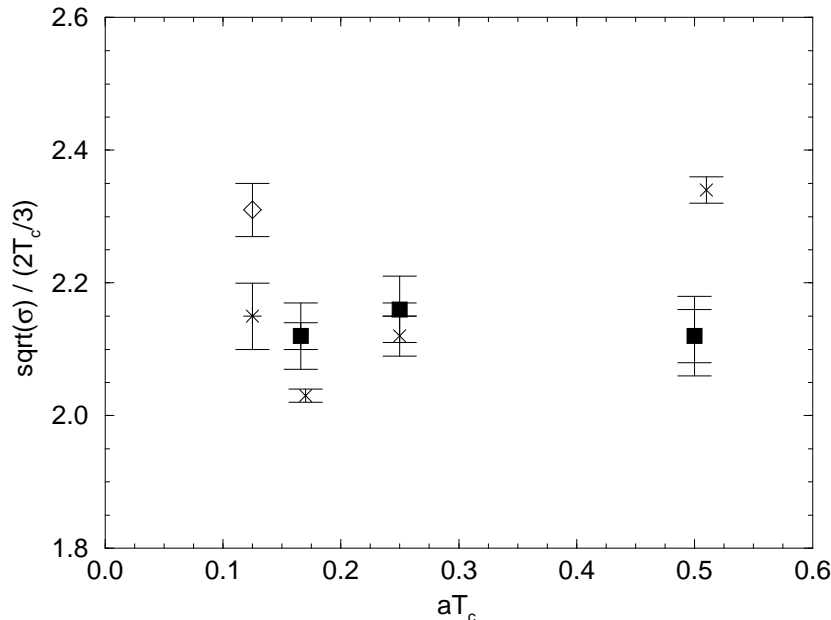


Figure 2: Scaling test for the Wilson action (crosses) and FP action (squares) on aspect ratio $3/2$ lattices. T_c is defined in infinite spatial volumes. The diamond is a Wilson action simulation by us at $\beta = 6.0$ and the star is an extrapolation using two-loop scaling to the correct (Ref. 8) $\beta_c = 6.06$.

Another scaling test is offered by the $q - \bar{q}$ potential $V(r; L)$ in a volume L^3 where L is chosen here to be $L = 2N_t$. Unfortunately, this quantity is contaminated by cut-off effects for $r \sim a$ coming from non-perfect *sources*. The FP Polyakov loop has not been constructed yet beyond the quadratic approximation (paper I), so we measured simple Polyakov loop correlations. The different

behaviour of the potentials obtained with the Wilson and FP actions is well demonstrated by Figs. 3 and 4, nevertheless.

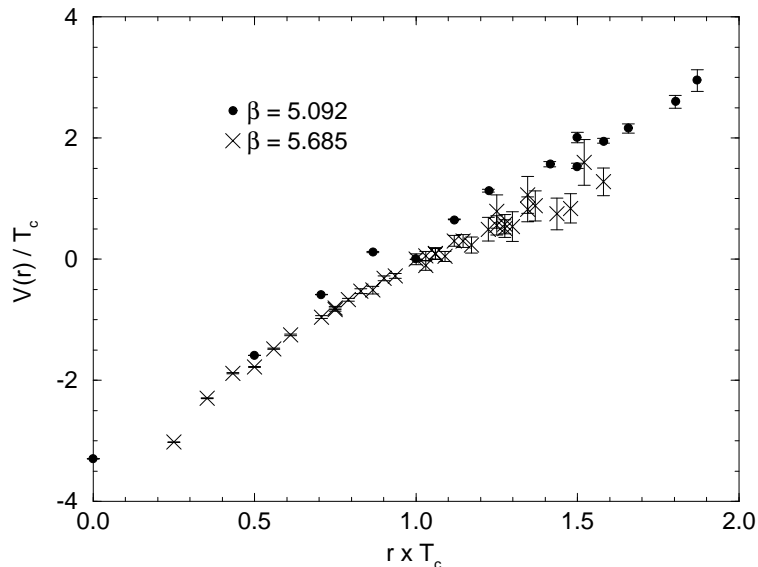


Figure 3: Potential $V(r)/T$ vs. rT for the Wilson action at $\beta_c(N_T = 2)$ (filled circles) and $\beta_c(N_T = 4)$ (crosses).

In the potential of the FP action the rotational symmetry violation at large r drops below the statistical errors even at $\beta_c(N_t) = 2$ but remains clearly present for the Wilson action. (Compare, for example, the predictions at $r = 1.5/T_c$ coming from $\vec{r} = (0, 0, 3)$ and $\vec{r} = (1, 2, 2)$ at $\beta_c(N_t) = 2$.) The non-physical additive constant in the potential was fixed by the convention $V(r = 1/T_c) = 0$. The lack of scaling for the Wilson action is evident, while the long distance behaviour of the potential is consistent with scaling for the 8 parameter FP action.

The outline of the paper is as follows: In Section 2 we describe the construction of a classical FP action which is appropriate for gauge configurations whose fluctuations are not small. In Section 3 we give an approximate simple parametrization of the FP action which represents the FP on gauge field configurations which are typical at the correlation lengths of our simulation. Finally, in Section 4 we give some details of the scaling tests using this action.

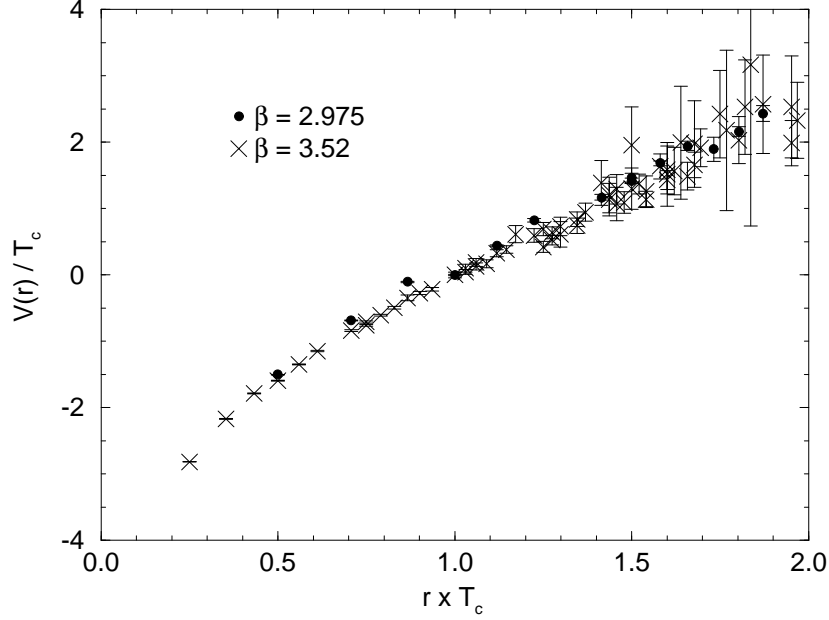


Figure 4: Potential $V(r)/T$ vs. rT for the FP action at $\beta_c(N_T = 2) = 2.975$ (filled circles) and $\beta_c(N_T = 4) = 3.52$ (crosses).

2 Numerical analysis of the FP equation and the problem of parametrization

We consider an $SU(N)$ pure gauge theory³ on the lattice and consider the RG transformation

$$e^{-\beta' S'(V)} = \int DU \exp \{-\beta (S(U) + T(U, V))\}, \quad (2)$$

where U is the original link variable, V is the blocked link variable and $T(U, V)$ is the blocking kernel that defines the transformation. At $\beta = \infty$ the transformation becomes a steepest decent relation

$$S^{FP}(V) = \min_{\{U\}} (S^{FP}(U) + T(U, V)), \quad (3)$$

where

$$T(U, V) = -\frac{\kappa}{N} \sum_{n_B, \mu} \left[\text{ReTr} (V_\mu(n_B) Q_\mu^\dagger(n_B)) - \max_W \{ \text{ReTr}(W Q^\dagger) \} \right]. \quad (4)$$

³The actual numerical analysis and simulations in this paper were done for $SU(3)$. The equations are written for general N if not indicated otherwise.

In Eq. (4) $W \in SU(N)$ and the $N \times N$ complex matrix $Q_\mu(n_B)$ is the block average. Its form depends on the block transformation. For the two different block transformations (type I and type II) which are considered here Q is defined in Figs. 5 and 6 in I. For further details we refer also to I.

In I we solved Eq. (3) up to cubic (quadratic) order in the vector potentials for type I (type II) block transformation. If the configuration V has large fluctuations one has to use numerical methods to solve the FP equation.

For numerical simulations we need a parametrization for the FP action which is sufficiently simple to make the computational overhead acceptable. It turns out, however, that the process of solving Eq. (3) requires, as an intermediate step, a more general parametrization. This is the problem we discuss first.

2.1 Parametrization of actions

Our parametrization is based on powers of the traces of the loop products $U_C = \Pi_C U_\mu(n)$ where C is an arbitrary closed path

$$S(U) = \frac{1}{N} \sum_C (c_1(C)(N - \text{ReTr}(U_C)) + c_2(C)(N - \text{ReTr}(U_C))^2 + \dots + d_2(C)(\text{ImTr}(U_C))^2 + d_4(C)(\text{ImTr}(U_C))^4 \dots). \quad (5)$$

We also checked other possibilities. The success of a parametrization of the σ -model and the form of exact classical solutions in both models suggest building gauge invariant quantities from U_C by using the angles after diagonalization, $U_C^{diag} = (e^{i\theta_1}, e^{i\theta_2}, e^{i\theta_3})$ for $N = 3$ [10]. For $SU(3)$ gauge theory this type of parametrization did not work better than the one in Eq. (5) and was, therefore, abandoned. We also tried to include the product of traces of different loops. It is quite difficult to keep track of the large number of topological possibilities and, in those cases we checked, the parametrization did not become better. The following results are based on the parametrization in Eq. (5).

Using optimized parameters in the block transformation the quadratic and cubic part of the FP action is short ranged (paper I). So, we decided to restrict the set of loops C to the 28 topologically different loops that are length 8 or less and fit into a 2^4 hypercube. They are tabulated in Table 3. Only 7 (15) of the 28 are independent on the quadratic (cubic) level. For the RG transformation of type I the FP action is known up to cubic order analytically which can be used to fix 15 of the $c_1(C)$ coefficients by a χ^2 fit. We decided to keep only 12 operators since the fit did not improve further. For the RG transformation of

type II 7 $c_1(C)$ couplings were fixed this way since the analytic cubic result is not available. Table 4 and Table 5 contain the $c_1(C)$ coefficients obtained. We shall denote the action where these couplings are kept only by S_q^{FP} .

Table 3: Loops used in the construction of the FP action. One particular orientation is shown; all possible orientations are included in the actual operators.

<i>label</i>	<i>path</i>
1	x,y,-x,-y
2	x,y,y,-x,-y,-y
3	x,y,z,-y,-x,-z
4	x,y,z,-x,-y,-z
5	x, y, x, y, -x, -y, -x, -y
6	x, y, x, y, -x, -x, -y, -y
7	x, y, x, z, -y, -x, -x, -z
8	x, y, x, z, -x, -z, -x, -y
9	x, y, x, z, -x, -y, -x, -z
10	x, y, x, z, -x, -x, -z, -y
11	x, y, x, -y, -x, y, -x, -y
12	x, y, y, x, -y, -x, -x, -y
13	x, y, y, z, -y, -z, -x, -y
14	x, y, y, z, -y, -y, -x, -z
15	x, y, y, z, -y, -x, -z, -y
16	x, y, y, z, -x, -y, -y, -z
17	x, y, y, -x, z, -y, -y, -z
18	x, y, y, -x, -x, -y, -y, x
19	x, y, z, t, -z, -t, -x, -y
20	x, y, z, t, -z, -y, -x, -t
21	x, y, z, t, -z, -x, -t, -y
22	x, y, z, t, -z, -x, -y, -t
23	x, y, z, t, -y, -x, -t, -z
24	x, y, z, t, -y, -x, -z, -t
25	x, y, z, t, -x, -y, -z, -t
26	x, y, z, -y, -z, y, -x, -y
27	x, y, z, -y, -x, y, -z, -y
28	x, y, -x, -y, x, y, -x, -y

2.2 Numerical minimization

To go beyond leading order we solved the fixed point equation Eq. (3) numerically. The procedure is the following: First we create an arbitrary SU(3) configuration $\{V\}$. That serves as a coarse configuration. Our goal is to find a

Table 4: Couplings of the fixed point action of Type I given in terms of loops defined in Table 3. The quadratic couplings are labelled by c_1 , and the coefficients of higher powers of $(3 - \text{Tr}U(C))$ from the fit described in Sec. 2.2 are also shown.

loop	c_1	c_2	c_3	c_4
1	.6744	.1067	-.1072	.0186
2	-.02	.0424	-.0304	.0055
3	.012	.0361	-.0228	.00436
4	.005	.1132	-.0632	.00937
5	-.0031	.0765	-.0562	.0109
8	-.0035	.00525	-.00418	.00076
9	.0027	.00402	-.00642	.00130
15	-.0024	-.0356	.0187	-.00268
16	.0013	-.0023	-.00373	.00132
20	.003	.0193	-.0119	.00211
23	.0032	.0187	-.0128	.0024
25	.0024	.0126	-.0115	.0021

fine configuration $\{U\}$ according to Eq. (3). Since we do not know S^{FP} (and even if we knew it, it presumably would be too complicated to use in a numerical minimization), we approximate S^{FP} with a simpler action S_0 . We choose S_0 such that it is sufficiently simple for minimization but close to the fixed point action. The minimization of Eq. (3) gives the fine configuration $\{U_0\}$ as a minimum

$$S'(V) = \min_U (S_0(U) + T(U, V)) = S_0(U_0) + T(U_0, V). \quad (6)$$

If S_0 is close to the fixed point action S^{FP} , then U_0 is close to $\{U^{FP}\}$ and up to quadratic corrections

$$\begin{aligned} S^{FP}(V) &= S^{FP}(U_0) + T(U_0, V) \\ &= S^{FP}(U_0) + (S'(V) - S_0(U_0)). \end{aligned} \quad (7)$$

This equation can be used to calculate the value of the fixed point action on the coarse configuration $\{V\}$ if S^{FP} is known on the fine configuration $\{U_0\}$.

One might think we got nowhere this way but this is not so. One observes that the minimizing configuration $U^{FP}(V)$ (which is close to $U_0(V)$) has much smaller fluctuations than the configuration V . As Eq. (4) shows, $T(U^{FP}(V), V)$ is non-negative and so Eq. (3) implies that $S^{FP}(V) \geq S^{FP}(U^{FP}(V))$. From this inequality it follows that the action density on the fine lattice is at least $1/2^4$ times smaller than on the coarse one. Actually, the observed ratio is even

Table 5: Couplings of the fixed point action of Type II, labeled as in Table 4 .

loop	c_1	c_2	c_3	c_4
1	.5454	-.0837	0.0459	-.0076
2	.0094	-.0335	.0161	-.0026
3	.0	.0639	-.0403	.0076
4	.0419	.0594	-.0485	.0091
5	.0	.0088	-.0060	.0010
8	.0	-.0022	.0008	-.0001
9	.0019	.0033	-.0019	.0003
17	-.0011	.0035	-.0015	.0002
18	-.0041	-.0081	.0040	-.0006
20	.0	-.0109	.0074	-.0011
23	.0	-.0213	.0111	-.0014
25	.0043	.0054	-.0039	.0007

smaller, it lies between $1/30$ and $1/50$ on the configurations we considered⁴. On the configurations $U_0(V)$ which have very small fluctuations the FP action can be replaced by S_q^{FP} defined at the end of Section 2.1⁵. Eq. (7) gives then the value of the FP action on the configurations V .

The procedure described above could fail if S_0 in the original minimization was not close to the FP action. We found that by carefully adjusting the couplings of S_0 one can make the difference $S^{FP}(U_0) - S_0(U_0)$, that measures this correction, small. After a certain amount of trial and error we were able to reduce these “perturbative” corrections to less than 0.4% and 0.3% of the action for the type I and type II RG transformations, respectively. In fig. 5 we illustrate this fact for the type I RGT.

In the case of the RG transformation of type I we generated about 400 configurations on 2^4 and 4^4 coarse lattices using the Wilson action, with coupling β ranging from 5.0 to 7.0. For type II we created more than 700 configurations in the coupling constant range 5.0 to 50.0. Following the steps of the discussion above we associated to each configuration a real number $S^{FP}(V)$, i.e. the value of the FP action on the configuration.

Our next task is to find a parametrization for S^{FP} which reproduces the action values to an acceptable accuracy and, at the same time, is sufficiently simple to be used in numerical simulations. This problem will be discussed in

⁴In order to appreciate how small is this ratio let us remark that the Wilson action density $(3 - \text{ReTr}U_P)$ is reduced by a factor of ~ 2 as β is changed from 5.0 to 10.0.

⁵One might and we did include further terms in order to cope with the small corrections which arise when V is very coarse and so the fluctuations of $U_0(V)$ are not so small anymore. In order to keep the discussion straight we do not follow this point further.

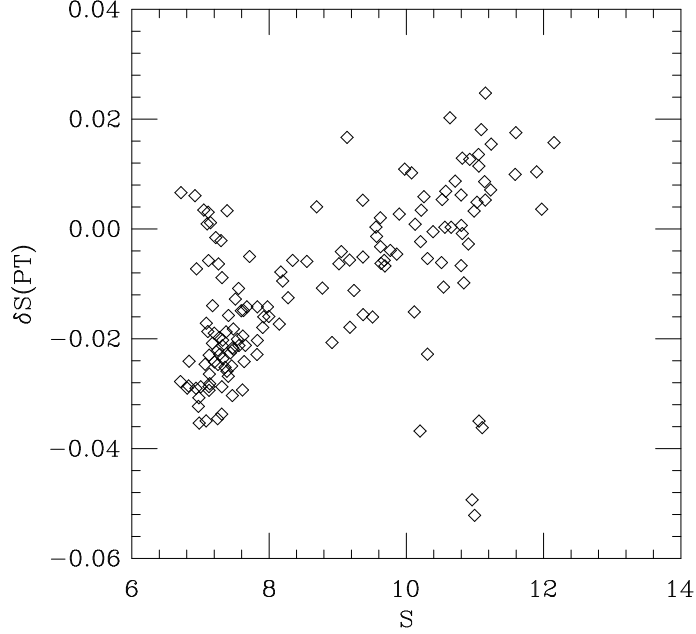


Figure 5: The perturbative corrections $\delta S_{PT} = S^{FP}(U_0) - S_0(U_0)$ for a set of configurations using the type I RGT.

Section 3. Beyond that we would like to make the information stored in the generated configurations and action values available to those who might want to create their own simple parametrization for simulations. For this purpose we parametrized S^{FP} as in Eq. (5) keeping a large number of loops from the set in Table 3. The couplings are presented in Table 4 and Table 5 for the RG transformations of type I and type II, respectively. Of course, these complicated actions are not practical to be used in simulations. They are used only to encode information which would be difficult to present otherwise. The actions in Table 4 and Table 5 satisfy the FP equation Eq. (3) on our configurations to a reasonable precision. The difference between the left and right hand sides of Eq. (3) is no more than 2% of the action, and in most of the cases the difference is much less. The quality of the fit is illustrated in fig. 6.

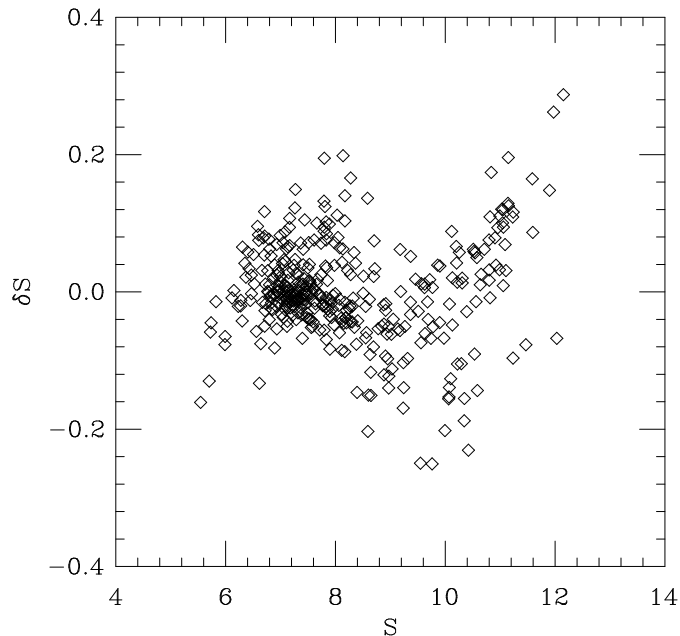


Figure 6: δS (the difference between the two sides of Eq. (3)) vs. S_{min} for the many parameter fit of Table 4 for the type I RGT.

2.3 Technical remarks on numerical minimization

In order to avoid programming errors two codes were written independently (this applies for all the essential parts of the numerical analysis presented in this paper). In both cases the lattice was swept through repeatedly, making a random local change and accepting the change if it lowered the action. The local change consisted a random rotation on a fine link, or on two neighbouring fine links at the same time. The rotations were parametrized and the action was interpolated quadratically in the parameters to find a set of values which minimized the action in this local few-parameter space. The configuration was overwritten only after checking that the action was really lowered.

In order to speed up the minimization process it was useful to begin with a fine configuration close to the final answer. One strategy for constructing such a configuration was to drop the $ReTrWQ^\dagger$ normalizing term from $T(U, V)$ during

the minimization and to relax for 20 to 50 sweeps. This typically brought the action to within ten per cent of its minimum value. Then 20 to 50 sweeps of the full minimization were required to achieve convergence at the fourth digit of accuracy. Another method was to build a fine starting configuration using the connecting matrix Z (Eq.(25) in I) valid on configurations with small fluctuations. This method, which required temporary gauge fixing, worked surprisingly well even on rough configurations.

3 The few-parameter FP action

For numerical simulation we need a parametrization which is simple and approximates the FP action sufficiently well on those configurations which are typical in the actual calculation. In order to find such a parametrization we used coarse configurations generated by the Wilson action between $\beta = 5.2$ and 6.0 and fitted $S^{FP}(V)$ with powers of the traces of only 2 loops.

The two loops we used in our few-parameter fit were the plaquette and loop #4 in Table 3, the twisted 6 link operator (x,y,z,-x,-y,-z). For RG transformation of type I we kept $c_i, i = 1, \dots, 4$ and put $d_i = 0$. The fit for the 8 parameters are listed in Table 1. For RG transformation of type II we parametrized with $c_i, i = 1, \dots, 5$ and $d_i, i = 1, \dots, 3$. The corresponding 16 fitted parameters are given in Table 2.

The accuracy of the fit is illustrated for the 8 parameter action in Fig. 7 where $\delta S = S^{fit}(V) - S^{FP}(V)$ is plotted as a function of S^{FP} . The quality of the fit deteriorates for smaller correlation lengths (larger S^{FP}) but remains within the 5% range.

As is evident from Tables 1 and 2, the FP action is dominated by the plaquette term with a small contribution of the 6 link operator in the lowest power. Can we neglect higher powers of loops altogether? To illustrate the importance of these small coefficients, in Fig 8 we plot $\delta S = S^{fit}(V) - S^{FP}(V)$ calculated with *only* the quadratic c_1 coefficients. It is obvious that the seemingly small $c_i, i = 2, 3, 4$ terms play a very important role in fitting the FP action.

The parameters in Tables 1 and 2 were chosen to approximate the FP action on configurations typical of a correlation length range occurring in $\beta_{Wilson} \sim (5.2, 6.0)$. If we wanted for some reason to perform simulations at 10^{-3} fm, we would use a parameterization of the FP action which was valid at the small lattice spacing.

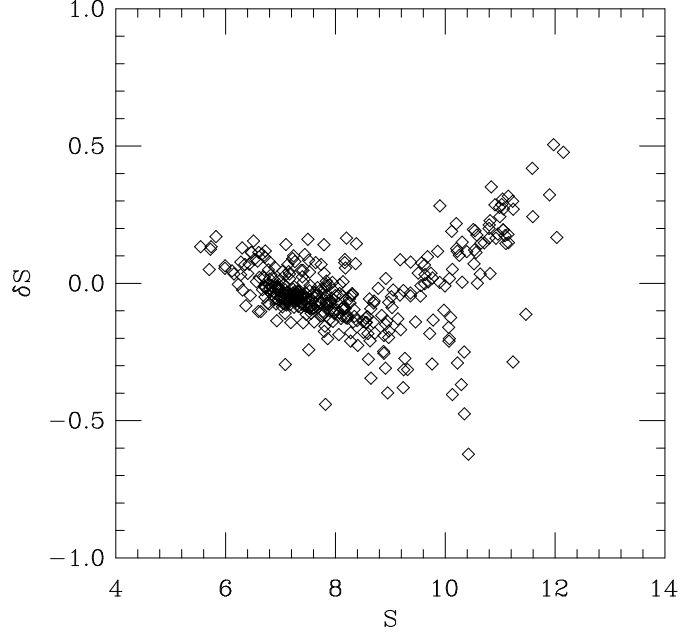


Figure 7: $\delta S = S^{fit}(V) - S^{FP}(V)$ vs. S^{FP} for the 8 parameter fit.

4 Simulations with approximate FP actions

The FP action is the classically perfect lattice action. As we argued in I, it is perfect even in 1-loop perturbation theory. These features make it plausible to expect that the FP action will have improved properties even at small correlation lengths. We present a detailed scaling test for the FP action of the RG transformation of type I using the approximate parametrization in Table 1.

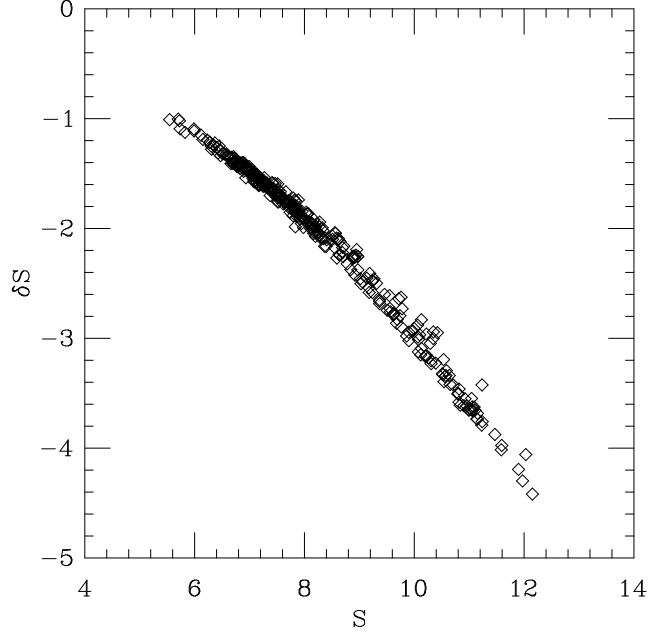


Figure 8: δS vs. S_{min} using *only* the quadratic coefficients of the action.

4.1 Simulation algorithms

We have adapted two algorithms for simulation. First, we have written a mixed Metropolis/overrelaxation algorithm which acts on $SU(2)$ subgroups, in complete analogy with a standard Wilson action code. No special optimization was done. The program runs with 8 parameters about a factor of 5 slower than with 1 parameter corresponding to the Wilson action. This latter is a factor of 1.4 slower than a highly optimized Wilson code. There are three reasons for the loss of speed. The first is the extra loops needed by the new action. The second is that because the action is not linear in a link variable, one cannot sum the links in the staples ahead of time, but must do so for each new update. Finally, again because the action is not linear in the link variables, we have not been able to

invent a microcanonical overrelaxation step, and after each overrelaxation step we must recompute the action and perform a Metropolis accept/reject step. The recomputation is unnecessary for the Wilson action. We have not precomputed any parts of the action for greater speed; the program is designed for arbitrary actions.

All our running on serial machines has used this algorithm. We typically do a mix of four overrelaxation updates on each of three $SU(2)$ subgroups on each link, followed by a one-hit Metropolis update (this is a “sweep” as used below), mimicking a conventional updating pattern for the Wilson action. We have not done long enough runs to have measured reliable simulation autocorrelation times. They appear to be about five sweeps for the plaquette, measured near the $N_t = 4$ critical coupling. The autocorrelation time was negligible for the correlators of Polyakov loops. We typically measure all quantities once per sweep. Of course, the whole point of the perfect action program is to be able to run on small lattices with small correlation lengths where critical slowing down is absent.

The overrelaxed/Metropolis algorithm is rather inconvenient for parallel machines. The action does not parallelize on two checkerboards due to the presence of the six-link term, and because the action includes more than loops in the fundamental representation, much temporary storage is needed. Neither problem is insurmountable, but we avoided them by using the Hybrid Monte Carlo algorithm [11]. The HMC code we have written for the eight-parameter FP action is about a factor of seven slower than a highly optimized Wilson action HMC code [12]. The difference in speed is easily understood as coming entirely from the many extra loop terms in the action.

4.2 The method of testing the FP action

When scaling holds the ratio of two physical masses is independent of the lattice resolution, which can be changed by tuning the coupling β . One of the physical masses we took is the critical temperature T_c which is used to set the physical scale. The lattice spacing a and T_c are related in the usual way, by finding the critical coupling $\beta_c(N_t)$ at which the confinement-deconfinement transition occurs on a lattice of size $N_s^3 \times N_t$ (with $N_s \gg N_t$). All our additional simulations were done at the discrete β values $\beta_c(N_t)$, where the lattice spacing is already fixed and given by $a = 1/(T_c N_t)$.

For the other physical mass we measured the torelon mass. A somewhat less quantitative test is offered by the potential which we also measured.

In the first case the scaling test is the quantity $G = L\sqrt{\sigma(L)}$ where $\sigma(L)$ is the string tension on an L^3 volume measured through the torelon mass. We performed the numerical experiment at two different aspect ratios $L/N_t = 2$ and $3/2$.

In the second case we studied the potential $V(r; L)$ in a volume L^3 , where L was chosen to be $L = 2N_t$. This test is less quantitative, since, rather than using FP Polyakov loops which we have not yet constructed beyond the quadratic approximation (paper I), the potential was extracted from simple Polyakov loop correlations. This is correct only for $r \gg a$ where it makes a negligible error that the Polyakov loops create sources whose distance is not exactly r .

4.3 Critical couplings for deconfinement

We found that the Columbia group's definition [13, 14] of β_c is the easiest to use on small volumes. Specifically, we make simulations of up to several tens of thousands of sweeps, recording the value of the real and imaginary parts of the Polyakov loop averaged over the lattice. We form the angle θ from $\tan \theta = \text{Im}P/\text{Re}P$ and measure the fraction of the time f_{20} that θ lies within ± 20 degrees of one of the ordered orientations expected for the Polyakov loop in the high temperature phase. We define β_c as the place where the deconfinement fraction

$$f_D = \frac{3}{2}f_{20} - \frac{1}{2} \quad (8)$$

equals fifty per cent. Most of our simulations are done on lattices of spatial size L between 2 or 3 times N_t . On these sizes close to β_c the lifetimes of the various Z_3 vacua average a few hundred sweeps. As we will see, it is necessary to measure β_c to within ± 0.005 to make meaningful scaling tests. We found alternate diagnostics such as histograms of the average Polyakov loop modulus just less precise than f_D measurements.

Infinite volume β_c values are found by extrapolating finite volume β_c values linearly in $1/\text{volume}$ and also by looking at crossings in a plot of Binder cumulants, which for us is $B = 1 - \langle L^4 \rangle / (3\langle L^2 \rangle^2)$, where L^2 is the absolute square of the volume-averaged Polyakov loop on a configuration, $L^4 = (L^2)^2$, and $\langle \rangle$ is an average over a simulation run.

We have measured critical couplings on lattices with $N_t = 2, 3, 4$, and 6 . The spatial volumes and critical couplings are shown in Table 6. Examples of plots of deconfinement fractions are shown in Fig. 9. A plot of β_c vs. $1/\text{volume}$ is shown in Fig. 10. Although the FP action is not designed to improve asymptotic scaling, just scaling, we can still see if asymptotic scaling obtains. Using the

original coupling in the action, we compute T_c/Λ from the two loop formula from our data, and record the results in Table 6 and Fig. 11. The eight parameter FP action not only shows asymptotic scaling within twenty per cent from $N_T = 2$ to 6 but in addition the value of its Λ parameter is about a factor of ten larger than the Wilson one and therefore much closer in value to the continuum Λ parameters.

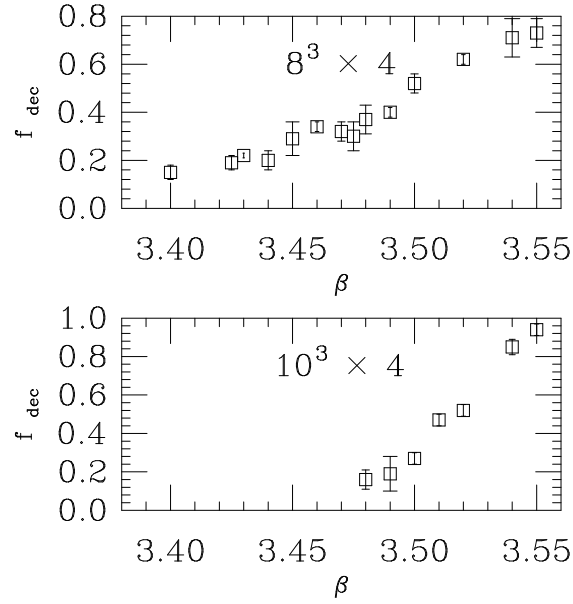


Figure 9: Deconfinement fractions for the eight-parameter FP action for $N_t = 4$ lattices.

Table 6: Critical couplings at finite volume and extrapolated to infinite volume for the FP action with parameters in Table 1.

volume	$N_t = 2$	$N_t = 3$	$N_t = 4$	$N_t = 6$
4^3	2.89(1)			
6^3	2.945(15)	3.320(15)		
8^3	2.96(1)	3.34(1)	3.50(1)	
10^3	2.960(5)	3.34(1)	3.51(1)	3.78(2)
12^3	2.975(5)	3.343(5)	3.520(5)	3.775(5)
15^3				3.777(5)
18^3				3.790(5)
infinite	2.976(5)	3.345(5)	3.520(5)	3.790(6)
T_c/Λ	7.68	7.61	6.87	6.13

4.4 Torelon masses

The string tension σ is measured through the correlator of pairs of Polyakov loops (or more complicated objects; see below): on a lattice of transverse size L the correlator of two Polyakov loops averaged over transverse separations and separated a longitudinal distance z is

$$C(z) = \sum_{r_\perp} \text{Re} \langle P_j(r_\perp, z) P_j^\dagger(0, 0) \rangle \simeq \exp(-\mu z), \quad (9)$$

where μ is the so-called torelon mass. On an infinite lattice $\mu = \sigma L$ and we will make the same definition on a finite lattice.

A problem with Polyakov loop correlators is that the signal to noise ratio rises exponentially with the string tension, L , and z : a simple calculation shows that with N measurements

$$\text{Signal/Noise} \simeq \sqrt{N} \exp(-\sigma L z). \quad (10)$$

Since as β falls, σ rises, this means that at small β it is difficult to observe a signal unless z is very small. However, at small z the signal may be contaminated by excited states, and it may be impossible to go to large enough z to be certain that one is seeing the asymptotic behavior of the signal before it disappears in the noise.

We are primarily interested in lattice spacings in the range $aT_c = 1/2$ to $1/8$ (for the Wilson action, $5.1 < \beta \leq 6.0$). At large lattice spacing ($aT_c = 1/2$) the best signals came from the Polyakov loop itself, measured with the Parisi – Petronzio – Rapuano [15] multihit variance reduction method. At smaller lattice spacing ($aT_c \leq 1/3$) the signal from this operator degrades and we had

more success using correlators of APE-blocked [16] links: we iterate

$$V_j^{n+1}(x) = (1 - \alpha)V_j^n(x) + \alpha/4 \sum_{k \neq j} (V_k^n(x)V_j^n(x + \hat{k})V_j^n(x + \hat{j})^\dagger + V_k^n(x - \hat{k})^\dagger V_j^n(x - \hat{k})V_j^n(x - \hat{k} + \hat{j})) \quad (11)$$

(with $V_j^0(x) = U_j(x)$ and $V_j^{n+1}(x)$ projected back onto $SU(3)$), with α varying from 0.2 at $aT_c = 1/3$ to 0.5 at $aT_c = 1/4$ to 0.7 at $aT_c = 1/8$ and the number of blocking steps rising from 10 to 15. Presumably a large part of the noise is local (in physical units) and hence more nonlocal (in units of a) averaging is needed as the lattice spacing falls.

The multihit algorithm is not very convenient when using the FP action on a parallel machine for the same reason that Metropolis or overrelaxation is inconvenient, but as we only ran the small lattice spacing simulations on parallel machines that is not a problem.

We determined the torelon mass from a single-exponential correlated fit, beginning at a minimum z where the χ^2/DF is near unity, and where we see stability in the effective mass over a range of z . At $aT_c = 1/2$ the fits are to $z = 1$ and $z = 2$ points only since there is no signal for $z > 2$.

As a check of our programs we reproduced the torelon mass measurements of Michael and Teper [17] on Wilson $\beta = 5.9$, 12^3 and $\beta = 6.0$, 16^3 lattices. At lower β there is little Wilson data for torelons which is a variational bound to which we can compare: at $\beta = 5.69$ our torelon mass is greater than the $\beta = 5.7$ result of de Forcrand et. al. [18] (which however was done using the non-variational cold wall source method.)

An uncertainty in the value of the critical coupling propagates into the uncertainty of G for the FP action. By doing lower-statistics simulations at couplings close to the critical β -values, we can roughly compute the variation of the torelon mass with β . For the uncertainties in β_c 's recorded in Table 6, this is an additional uncertainty in G of about 0.04–0.05 at $r = 2$ and $r = 3/2$. We include this uncertainty in the figures by combining it in quadrature with the statistical fluctuation in G ; in the figures the extreme range of the vertical error bars shows the combined uncertainty.

The result of our simulations is that the torelon mass measured on aspect ratio 2 lattices using the FP action scales within the statistical errors for $1/4 \leq aT_c \leq 1/2$, at a value which is consistent with the value inferred from Wilson action results from small lattice spacing simulations.

As a second test of scaling we compare torelon masses measured on lattices

Table 7: Our measurements of torelon masses from the Wilson action on small lattices.

volume	β	$\mu = L\sigma$	$L\sqrt{\sigma}$
$3^3 \times 16$	5.10	1.83(3)	2.34(2)
$4^3 \times 16$	5.10	2.86(6)	3.38(4)
$6^3 \times 16$	5.55	1.65(5)	3.15(5)
$6^3 \times 16$	5.69	0.75(2)	2.12(3)
$8^3 \times 16$	5.69	1.11(2)	2.98(3)
$9^3 \times 16$	5.9	0.45(1)	2.03(1)
$12^3 \times 16$	6.0	0.44(1)	2.31(4)

Table 8: Our measurements of torelon masses from the FP action.

volume	β	$\mu = L\sigma$	$L\sqrt{\sigma}$
$3^3 \times 12$	2.975	1.50(6)	2.12(4)
$4^3 \times 8$	2.975	2.38(5)	3.09(3)
$6^3 \times 12$	3.34	1.55(5)	3.05(5)
$6^3 \times 12$	3.52	0.78(1)	2.16(1)
$8^3 \times 12$	3.52	1.19(4)	3.08(4)
$9^3 \times 16$	3.79	0.50(1)	2.12(2)

of constant aspect ratio $3/2$. The scaling plot is shown in Fig. 2. In this figure the diamond shows the result of our simulation with the Wilson action at $\beta = 6.0$ and the star shows an extrapolation to $\beta_c(N_t = 8) = 6.06$ using asymptotic freedom. All the simulations were performed by us. Again, the FP action torelon mass scales for $1/6 \leq aT_c \leq 1/2$, while the Wilson action exhibits considerable scaling violation over the same range of lattice spacings.

4.5 The potential

Finally, we have measured the potential from the correlation function of Polyakov loops. The results obtained at $\beta_c(N_t = 2)$ and $\beta_c(N_t = 4)$ are shown in Figs. 3 and 4 for the Wilson and the 8 parameter FP actions, respectively. At large distances the system should forget the errors related to the bad operators and rotational symmetry has to be recovered. For the Wilson action at $N_t = 2$ strong symmetry violation is seen even at $rT_c = 1.5$ and there is a clear scaling violation in the long distance part of $V(r)$. These cut-off effects drop below the statistical errors for the FP action.

5 Conclusions

We have described a systematic program for constructing fixed point actions for SU(3) gauge theory, and illustrated it using a particular scale two blocking transformation. An approximation to the FP action shows scaling within our small statistical errors beginning at $aT_c = 1/2$, as compared to $aT_c \leq 1/8$ for the Wilson action, at a cost of a factor of about 7 in computational speed per site update.

This work allows one to consider a large number of questions.

First, the action which is simulated here and shows scaling is an approximation to a FP action, not to an action lying on any known renormalized trajectory at small β . Can one find the renormalized trajectory of these renormalization group transformations? We believe that this is feasible using the available techniques [19]. As a related question, the FP action scales for β values at which it was not a good fit to the FP action. It would be useful to understand how imperfect an action can be and still perform well. Additionally, it might be that completely different scale transformations, such as the $\sqrt{3}$ transformation [20], might yield FP actions which are even more local than this one.

In the meantime, the fixed point action can be used for many phenomenological calculations at large lattice spacing.

A particularly severe and unexpected bottleneck in this calculation was the absence of good scaling tests using the Wilson action. We are particularly hampered by imprecision in published values of deconfinement couplings for $N_t \geq 8$. We urge groups doing simulations with the Wilson action to choose parameters which are easy to relate to other length scales. We would also like to encourage developers of alternative improved actions to test them at very large values of the lattice spacing, since either scaling violations will be large and easy to see, or they will be small, showing that the candidate action is indeed an improvement.

Finally we would like to comment on lattice perturbation theory. The construction of the FP actions we have described here does not involve lattice perturbation theory in the sense that we have made no expansions in g^2 or in powers of the lattice spacing a . The actions themselves are not explicitly designed to have good perturbative expansions, although the one we have tested most extensively probably does so in terms of its bare coupling (since it seems to scale asymptotically with a small T_c/Λ ratio). Perturbative calculations for these actions are unpleasant but not impossible, given symbolic manipulation programs. Direct numerical calculations of renormalization constants [21] are

in principle no more difficult than for the Wilson action, although the currents themselves must be “perfect.”

These actions appear to open the way towards doing QCD simulations with modest computer resources.

6 Acknowledgements

U. Wiese participated in the early stages of this project. We would like to thank T. Barker, M. Horanyi and the Colorado high energy experimental group for allowing us to use their work stations. Some computations were performed on the Paragon at the San Diego Supercomputer Center and on the T3D at NERSC, Livermore. We want to thank P. Büttiker, M. Egger and M. Willers for their support in using the computing facilities at the University of Bern. T. D. would like to thank C. DeTar and U. Heller for discussions about measuring string tensions and D. Toussaint for help with the code. This work was supported by the U.S. Department of Energy and by the National Science Foundation and by the Swiss National Science Foundation.

A Appendix

We discuss here briefly the arguments which show that the numerical analysis of the classical FP equation Eq. (3) can be done on small lattices.

Consider a lattice of size $(mL)^4$ onto which a periodic L^4 coarse V configuration is copied m^4 times, where m is a large integer. The corresponding minimizing configuration $U_0(V)$ lives on an $(2mL)^4$ lattice. The fine links $U_\mu(n)$ and $U_\mu(n+2L\hat{\nu})$ are influenced identically by the coarse field V . Assuming that this symmetry is not broken spontaneously, the minimizing configuration will be periodic with period $2L$. The relation between the coarse field and the minimizing fine field on the big lattices is fixed by the relation between the L^4 and $(2L)^4$ lattice. On the other hand, the big $(mL)^4$ configurations are certainly legitimate candidates to be used to parametrize the FP action, since Eq. (3) should be satisfied on any type of V configurations.

The question remains whether the specific configurations considered above give sufficient information to fix the coefficients in Eq. (5). In spin models it is easy to see that solving the FP equation on small lattices one is not able

to resolve certain couplings in the FP action. Working on a 2^2 lattice in the non-linear σ -model, for example, one can not separately determine the two-spin couplings $\rho(1, 0), \rho(3, 0), \rho(5, 0), \dots$ – only their sum enters. Using a limited number of loops in a non-Abelian gauge theory on a small lattice it is not clear whether such relations exist. We emphasize, however that even if they exist, no error is caused by small lattices, only information is lost. Since the general parametrization in terms of loops is highly redundant and our specific parametrization is not at all systematic, this is not a real problem.

References

- [1] T. DeGrand, A. Hasenfratz, P. Hasenfratz, F. Niedermayer, preprint COLO-HEP-361, BUTP-95/14. This paper is referred to as I in the text.
- [2] P. Hasenfratz and F. Niedermayer, Nucl. Phys. B414 (1994) 785; P. Hasenfratz, Nucl. Phys. B (Proc. Suppl) 34 (1994) 3; F. Niedermayer, *ibid.*, 513.
- [3] G. Parisi, in the Proceedings of the XX International Conference on High Energy Physics, L. Durand and L. Pondrom, eds., American Institute of Physics, p. 1531.
- [4] G. P. LePage and P. Mackenzie, Phys. Rev. **D48** (1993) 2250.
- [5] C. T. H. Davies, K. Hornbostel, A. Langnau, G. P. Lepage, A. Lidsey, J. Shigemitsu, and J. Sloan, Phys. Rev. **D50** (1994) 6963; J. Sloan, Nucl. Phys. B (Proc. Suppl.) 42 (1995) 171.
- [6] A. Gall, “Strong coupling expansion with multiparameter action in the non-linear σ -model”, diplome work, Univ. Bern (1995), unpublished.
- [7] We used the tables of J. Fingberg, U. Heller, and F. Karsch, Nucl. Phys. B392 (1993) 493.
- [8] G. Boyd, et. al., Bielefeld preprint BI-TP 95/23, June 1995.
- [9] M. Lüscher, K. Symanzik and P. Weisz, Nucl. Phys. B173 (1980) 365, Ph. de Forcrand, G. Schierholz, H. Schneider and M. Tepper, Phys. Lett. B160 (1985) 137.
- [10] N. Manton, Phys. Lett. 96B (1980) 328
- [11] S. Duane, A. Kennedy, B. Pendleton, and D. Roweth, Phys. Lett. 194B, 271, 1987.

- [12] C. Bernard, T. DeGrand, C. DeTar, S. Gottlieb, A. Krasnitz, M.C. Ogilvie, R.L. Sugar, and D. Toussaint, in *Workshop on Fermion Algorithms*, edited by H. J. Hermann and F. Karsch, (World Scientific, Singapore, 1991).
- [13] N. Christ and A. Terrano, Phys. Rev. Lett. 56, 111(1986).
- [14] D. Toussaint, in the Proceedings of Lattice '86, H. Satz, et. al., eds., Plenum, 1987, p. 399.
- [15] G. Parisi, R. Petronzio, F. Rapuano, Phys. Lett. 128B, 418 (1983).
- [16] M. Falcioni, M. Paciello, G. Parisi, B. Taglienti, Nucl. Phys. B251[FS13], 624 (1985). M. Albanese, et. al. Phys. Lett. B192, 163 (1987).
- [17] C. Michael and M. Teper, Nucl. Phys. B314 (1989) 347.
- [18] Ph. de Forcrand, G. Schierholz, H. Schneider, and M. Teper, Phys. Lett. 160B (1985) 137.
- [19] M. Creutz, A. Gocksch and M. Ogilvie, Phys. Rev. Lett. 53 (1984) 875; M. Hasenbusch, K. Pinn and C. Wiecekowskiski, Phys. Lett. B338 (1994) 308; M. Hasenbusch, K. Pinn and C. Wiecekowskiski, Nucl. Phys. B (Proc. Suppl.) 42 (1995) 808; QCD-TARO Collaboration, Nucl. Phys. B (Proc. Suppl.) 42 (1995) 805.
- [20] R. Gupta, G. Kilcup, A. Patel, and S. Sharpe, Phys. Lett. B211 (1988) 132.
- [21] G. Martinelli, et. al., Nucl. Phys. B (Proc. Suppl.) 34, (1994) 507; preprint CERN-TH.7342/94; Nucl. Phys. B (Proc. Suppl.) 42 (1995) 428.

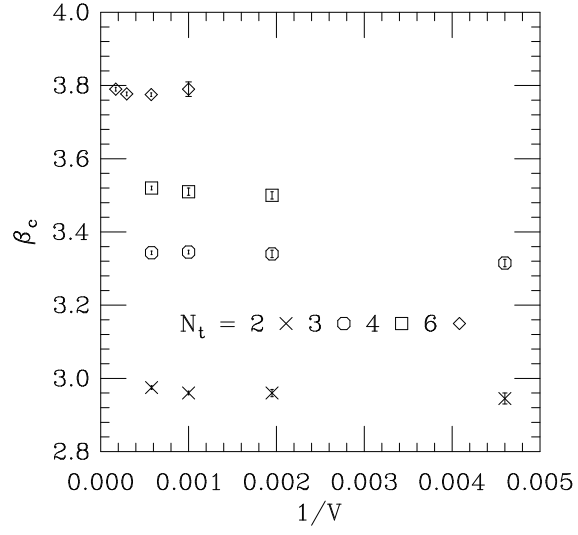


Figure 10: Volume dependence of critical couplings for the eight parameter FP action, and their extrapolations to infinite volume.

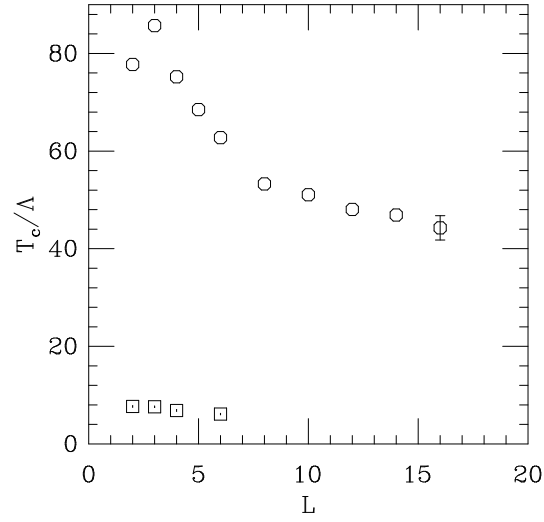


Figure 11: T_c/Λ for the Wilson (octagons) and FP (squares) actions.